Synthetic Strategies towards C_{70}: Molecular Mechanics and MNDO Calculations on Pinakene, $C_{28}H_{14}$ and Related Molecules

Eluvathingal D. Jemmis,* G. Narahari Sastry and Goverdhan Mehta*
School of Chemistry, University of Hyderabad, Central University, PO 500 134, Hyderabad, India

Molecular mechanics (MM2) calculations have been performed to estimate the strain energies of hydrocarbons derived from the fragments of C_{70} which retain C_5 or C_2 symmetry. There are two ways of dissecting C_{70} retaining C_2 symmetry, $C_2(a)$ and $C_2(b)$. The key fragment along the $C_2(a)$ route is pinakene, $C_{28}H_{14}$ (**12**). It exists in a bowl shape. Its strain energy is close to that of the corresponding C_{28} fragment of C_{70}. The bowl depth was calculated to be 2.03 Å at the MNDO level, and the 'bowl-to-bowl' inversion barrier calculated to be about 48.6 kcal mol^{-1}, implying that this is a very rigid bowl. The strain energy build-up from the sequential placement of methylene bridges in going from dibenzo[*fg,op*]naphthacene (**26**) to pinakene was estimated. Methyl derivatives of dibenzo-[*fg,op*]naphthacene were taken as the key precursors in this study. Strain energies of various positional isomers were also evaluated. Synthetic strategies towards pinakene are delineated.

Methods for the mass production of fullerenes are rapidly improving. Soot extraction and arcing or irradiation with sunlight on graphite are the methods available for the generation of fullerenes.[1] Predominant products of these processes are C_{60} and C_{70}, with smaller amounts of other carbon clusters.[1] The unusual chemical and physical properties of C_{60} have already made this material a centre of chemical activity in a short time.[2] Even though C_{70} is thermodynamically more stable than C_{60},[3] the latter is found in larger proportions.[1,2] Rational synthetic attempts towards fullerenes have already begun.[4–9] Our interest in exploring synthetic avenues to C_{60} led us to examine similar approaches towards C_{70} and its analogues.[4] Often the sub-structures of the fullerenes in general and the bowl-type molecules in particular provide fascinating chemistry.[4,7,10]

In a stepwise synthesis it is important to know the increase in strain associated with each step. Pathways that involve unusual strain build-up may then be avoided. In this paper we study the build-up of strain in sequential synthetic approaches to C_{70} using empirical force field calculations.[11] C_{70} can be dismantled retrosynthetically to give bowl- and ribbon-shaped structures. Removing fragments successively from one end whilst retaining a symmetry element—C_5 or C_2—gives bowl-shaped structures. There are two different retrosynthetic pathways possible if C_2 symmetry is retained in the process, as shown in Scheme 1. Let us call them $C_2(a)$ and $C_2(b)$. The σ-valency on the C_n fragment is then saturated by adding hydrogens. The hydrocarbons thus formed are treated as substructures of C_{70} (**1**) throughout this paper.

Pinakene,† $C_{28}H_{14}$ (**12**) is the smallest molecule along the $C_2(a)$ route which exists in the bowl form and naturally constitutes a stepping stone to the curved carbon networks of C_{70}. The fragments along the C_5 axis are very similar to those of C_{60}. We are interested mainly in the key substructures along the C_2 axis which are unique for C_{70}.

The ribbon-like substructures are arrived at by knocking off the fragments in pairs from opposite ends, and are depicted in Fig. 1. Ribbons along the C_5 route, **18–21**, result by removing identical units from top and bottom whereas those along the C_2 route are obtained by removal of non-equivalent units from top and bottom. The C_n skeleta along the C_5 route, **19–21**, have

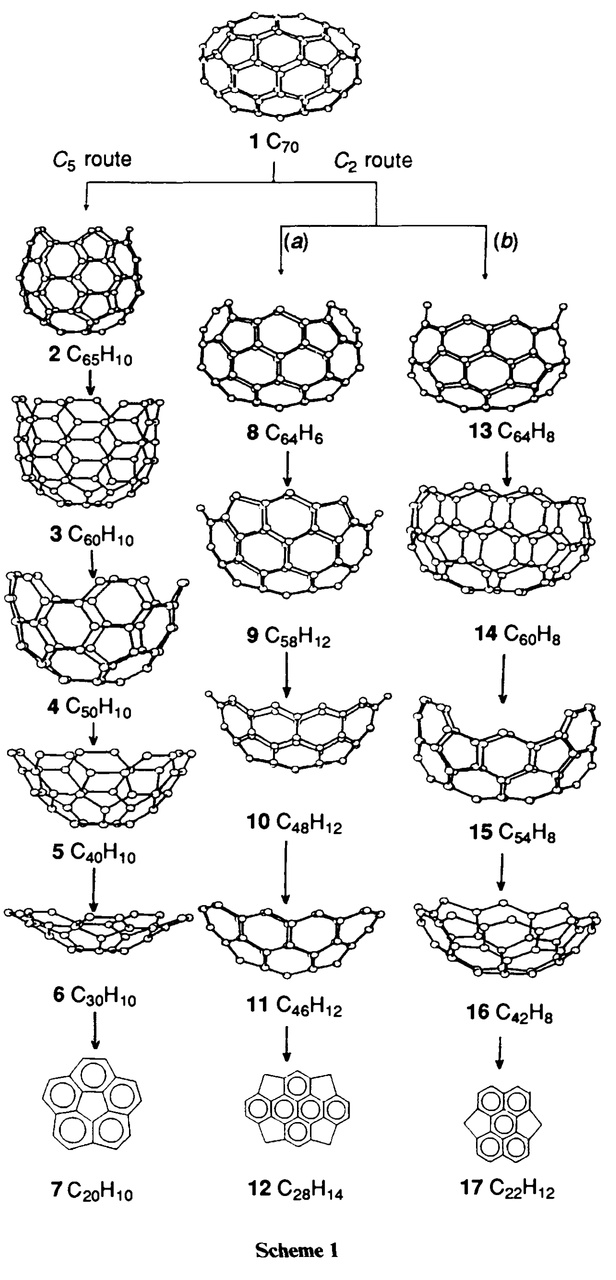

Scheme 1

---

† We bestow the trivial name 'pinakene' on this novel hydrocarbon, based on the Sanskrit word 'pinak' meaning a 'bow' describing a curved surface.

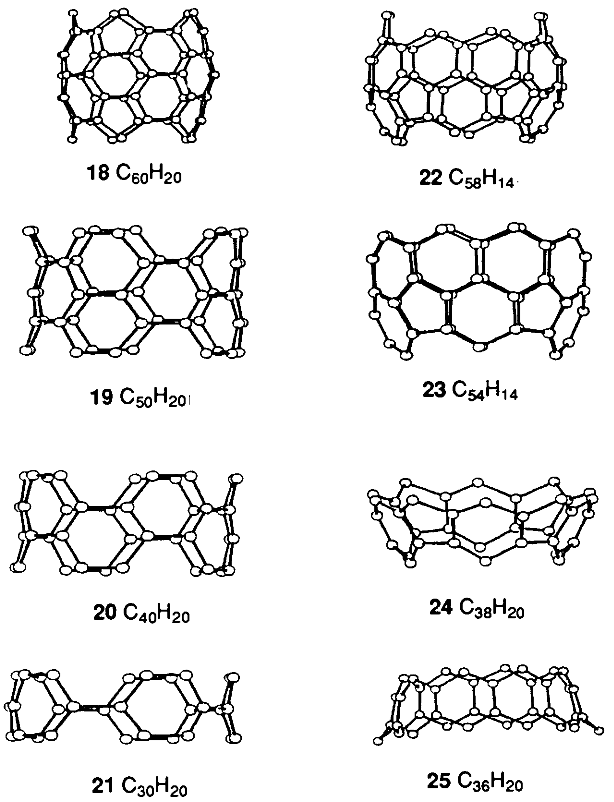
18 $C_{60}H_{20}$ **22** $C_{58}H_{14}$

19 $C_{50}H_{20}$ **23** $C_{54}H_{14}$

20 $C_{40}H_{20}$ **24** $C_{38}H_{20}$

21 $C_{30}H_{20}$ **25** $C_{36}H_{20}$

Fig. 1

been previously mentioned as substructures of C_{70}.[12] Of these, **20** and **21** are common to C_{60} and C_{70}. The syntheses of these ribbon-type molecules are highly challenging. They can be looked at as lower analogues of beltenes.[13] The six-membered rings are positioned horizontally in **18**–**21** and vertically in **22**–**25**. We evaluated the strain energies of various bowl- and ribbon-shaped fragments of C_{70} (**2**–**25** of Scheme 1 and Fig. 1) using molecular mechanics (MM2) calculations. The MNDO[14] study on **12** was carried out to determine the details of the geometry and the depth of the bowl. We explored the stepwise increase in the strain in going from dibenzo[*fg*,*op*]naphthacene, **26**, to **12**. Strategically, methylated derivatives of **26** are used as precursors here, which could form methylene bridge(s) upon flash vacuum thermolysis. Various isomers based on the position of the methyl groups were considered and schemes for the synthesis of C_{70} along this pathway are delineated at the end.

Results and Discussion

Molecular Mechanics Analysis.—The strain energies of the fragments **2**–**25** were evaluated using MM2 calculations with standard parameters (see Table 1). Comparison amongst fragments of various sizes was made possible by evaluating strain energy per carbon (E_S). The strain energies of the corresponding C_n fragments in an idealized C_{70} geometry were also calculated for comparison. The difference in strain energy between the optimized hydrocarbon and the corresponding C_n fragment of C_{70} was estimated (ΔE_S). This value roughly corresponds to the deviation of the particular hydrocarbon skeleton from that of the corresponding C_n fragment of C_{70}, but note that occasionally, addition of hydrogens to complete the valency added on significantly to the strain. E_S was found to be much lower for C_{70} than for C_{60}, indicating greater stability of C_{70}. The C_{70} fragments along the C_5 route are identical to those of C_{60}, except $C_{65}H_{10}$ (**2**) and $C_{60}H_{10}$ (**3**). In this pathway, there is a maximum at $C_{40}H_{10}$ (**5**). The strain energy of **5** is higher than the corresponding C_{40} skeleton of C_{70}.

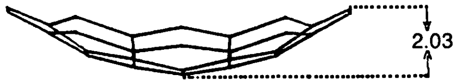

Fig. 2 MNDO optimized geometry of **12** showing the bowl depth (Å)

Pinakene (**12**) has substantial strain. The strain energy difference between **12** and the corresponding C_{28} fragment is only 2.78 kcal mol^{-1}.* The corresponding differences for $C_{20}H_{10}$ (**7**) and $C_{22}H_{12}$ (**17**) are 6.34 and 4.00 kcal mol^{-1}, respectively. $C_{22}H_{12}$ (**17**) is calculated to be planar both at molecular mechanics and MNDO levels. Obviously **12** is closer to the C_{70} (**1**) skeleton and a better target *en route* to C_{70}.

ΔE_S values of the ribbons along the C_5 route, **18**–**21**, present several interesting aspects. Major reorganization takes place in the larger ribbons $C_{60}H_{20}$ (**18**) and $C_{50}H_{20}$ (**19**). Comparatively, $C_{40}H_{20}$ (**20**) is closer in strain energy to C_{70}. The ΔE_S value for $C_{30}H_{10}$ is negative, indicating that hydrogens added to complete the valency bring in significant strain. However, the optimized carbon skeleton of $C_{30}H_{20}$ (**21**) resembles C_{70} (**1**). Ribbons along the C_2 route, **22**–**25**, have ΔE_S values around 2 kcal mol^{-1}. Hence, the reorganization of C_n skeleta in the optimized structure is comparable in molecules **22**–**25**. Though each of these ribbons is interesting in its own right, we do not discuss them any further here.

The Structure of $C_{28}H_{14}$.—We have studied structure, bowl depth and rigidity (bowl-to-bowl inversion barrier) of the fascinating molecule $C_{28}H_{14}$ to aid in devising synthetic strategies towards it and its further elaboration to C_{70}.

$C_{28}H_{14}$ is calculated to be bowl-shaped by the semiempirical MNDO method. The MNDO-optimized structure (**12**) is given in Fig. 2. The calculated bowl depth is 2.03 Å. We compare the bond lengths of $C_{28}H_{14}$ with those of **26**, obtained by removing the methylene bridges from $C_{28}H_{14}$, in Table 2 which gives the MNDO bond lengths of **26** and $C_{28}H_{14}$ in its planar (**12a**) and

Table 1 Strain energies of C_{70} fragments (all values are in kcal mol^{-1})

No.	Formula	E_S	E_S of C_n in C_{70}	ΔE_S
1	C_{70}	17.27		
2	$C_{65}H_{10}$	13.76	15.31	1.55
3	$C_{60}H_{10}$	12.53	14.20	1.67
4	$C_{50}H_{10}$	13.38	14.01	0.54
5	$C_{40}H_{10}$	14.43	14.19	−0.24
6	$C_{30}H_{10}$	8.83	13.52	4.69
7	$C_{20}H_{10}$	4.30	10.64	6.34
8	$C_{64}H_6$	15.83	15.98	0.15
9	$C_{58}H_{12}$	12.54	14.70	2.16
10	$C_{48}H_{12}$	12.30	13.66	1.36
11	$C_{46}H_{12}$	10.24	12.95	2.71
12	$C_{28}H_{14}$	7.39	10.17	2.78
13	$C_{64}H_8$	15.79	16.06	0.37
14	$C_{60}H_8$	14.72	15.12	0.40
15	$C_{54}H_8$	14.23	14.52	0.29
16	$C_{42}H_8$	10.43	12.51	2.08
17	$C_{22}H_{12}$	4.16	8.16	4.00
18	$C_{60}H_{20}$	9.79	13.16	3.37
19	$C_{50}H_{20}$	6.05	10.02	3.97
20	$C_{40}H_{20}$	6.65	8.74	2.09
21	$C_{30}H_{20}$	7.83	6.25	−1.58
22	$C_{58}H_{14}$	12.48	14.48	2.00
23	$C_{54}H_{14}$	12.20	13.32	1.12
24	$C_{38}H_{20}$	7.63	9.38	1.75
25	$C_{36}H_{20}$	7.13	9.39	2.26

---

* Non-S.I. unit employed: 1 cal = 4.18 J.

Table 2 MNDO bond lengths (Å) of $C_{24}H_{14}$ (**26**), $C_{28}H_{14}$ (planar) (**12a**) and $C_{28}H_{14}$ (bowl) (**12**). The numbering convention is as illustrated

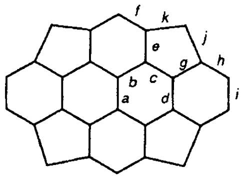

Bond type	$C_{24}H_{14}$ **26**	$C_{28}H_{14}$ (planar) **12a**	$C_{28}H_{14}$ (bowl) **12**
a	1.465	1.429	1.468
b	1.437	1.377	1.411
c	1.475	1.430	1.449
d	1.429	1.384	1.385
e	1.416	1.402	1.424
f	1.398	1.453	1.424
g	1.427	1.400	1.422
h	1.395	1.421	1.404
i	1.408	1.466	1.445
j		1.593	1.545
k		1.597	1.555

Table 3 Strain energies (in kcal mol^{-1}) of precursors of $C_{28}H_{14}$ starting from dibenzo[*fg*,*op*]naphthacene (**26**). Entry —B— against a pair of numbers indicate that a methylene bridge is formed between those sites. Entries M and H against a number correspond to methyl and hydrogen groups at that site. Valence isomeric forms used in all the molecular mechanics calculations are the same as those shown here. The numbering scheme employed is shown.

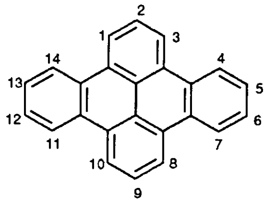

No.	14	1	11	10	7	8	4	3	E_S
26	H	H	H	H	H	H	H	H	58.7
12	—B—		—B—		—B—		—B—		206.4
27a	M	H	H	H	H	H	H	H	65.4
27b	H	M	H	H	H	H	H	H	65.4
28a	H	M	M	H	H	H	H	H	72.1
28b	H	M	H	H	H	H	H	M	71.0
28c	M	H	M	H	H	H	H	H	73.0
28d	M	H	H	H	H	M	H	H	71.3
28e	M	H	H	H	H	H	M	H	71.2
28f	H	M	H	M	H	H	H	H	71.0
28g	H	M	H	H	H	M	H	H	71.1
29a	M	H	M	H	M	H	H	H	77.8
29b	M	H	M	H	H	M	H	H	77.5
29c	M	H	H	M	H	M	H	H	76.8
29d	H	M	H	M	H	M	H	H	75.9
30a	M	H	M	H	M	H	M	H	83.1
30b	H	M	M	H	M	H	H	M	81.7
30c	H	M	H	M	M	H	M	H	81.6
30d	H	M	H	M	H	M	H	M	82.2
30e	M	H	H	M	M	H	H	M	83.4
30f	H	M	H	M	M	H	H	M	81.0
30g	M	H	H	M	M	H	M	H	82.5
31	—B—		H	H	H	H	H	H	67.2
32a	—B—		M	H	H	H	H	H	71.7
32b	—B—		H	M	H	H	H	H	72.6
32c	—B—		H	H	M	H	H	H	75.4
32d	—B—		H	H	H	M	H	H	75.6
32e	—B—		H	H	H	H	M	H	75.5
32f	—B—		H	H	H	H	H	M	75.0
33a	—B—		M	H	M	H	H	H	78.5
33b	—B—		M	H	H	M	H	H	78.4
33c	—B—		H	M	H	M	H	H	79.3
33d	—B—		H	H	M	H	M	H	84.3
33e	—B—		H	H	M	H	H	M	81.7
33f	—B—		M	H	H	H	H	M	78.0
33g	—B—		H	M	M	H	H	M	79.1
33h	—B—		M	H	H	H	M	H	78.5
33i	—B—		H	M	M	H	H	H	79.4
34a	—B—		M	H	M	H	M	H	82.5
34b	—B—		M	H	M	H	H	M	84.8
34c	—B—		M	H	H	M	H	M	85.5
34d	—B—		H	M	H	M	H	M	86.5
34e	—B—		H	M	H	M	M	H	85.8
34f	—B—		H	M	M	H	M	H	85.4
35	—B—		—B—		H	H	H	H	107.5
36a	—B—		—B—		M	H	H	H	111.0
36b	—B—		—B—		H	M	H	H	112.0
37a	—B—		—B—		M	H	M	H	118.5
37b	—B—		—B—		M	H	H	M	116.2
37c	—B—		—B—		H	M	H	M	117.4
38	—B—		H	H	—B—		H	H	80.2
39a	—B—		M	H	—B—		H	H	83.5
39b	—B—		H	M	—B—		H	H	84.1
40a	—B—		M	H	—B—		M	H	82.3
40b	—B—		M	H	—B—		H	M	82.5
40c	—B—		H	M	—B—		H	M	82.8
41	—B—		H	H	H	H	—B—		87.6
42a	—B—		M	H	H	H	—B—		89.3
42b	—B—		H	M	H	H	—B—		89.7
43a	—B—		M	H	M	H	—B—		91.2
43b	—B—		H	M	M	H	—B—		91.6
43c	—B—		H	M	H	M	—B—		92.1
44	—B—		—B—		—B—		H	H	136.7
45a	—B—		—B—		—B—		M	H	136.3
45b	—B—		—B—		—B—		H	M	136.5
46	—B—		—B—		—B—		—B—[a]		157.2

[a] Ethano bridge.

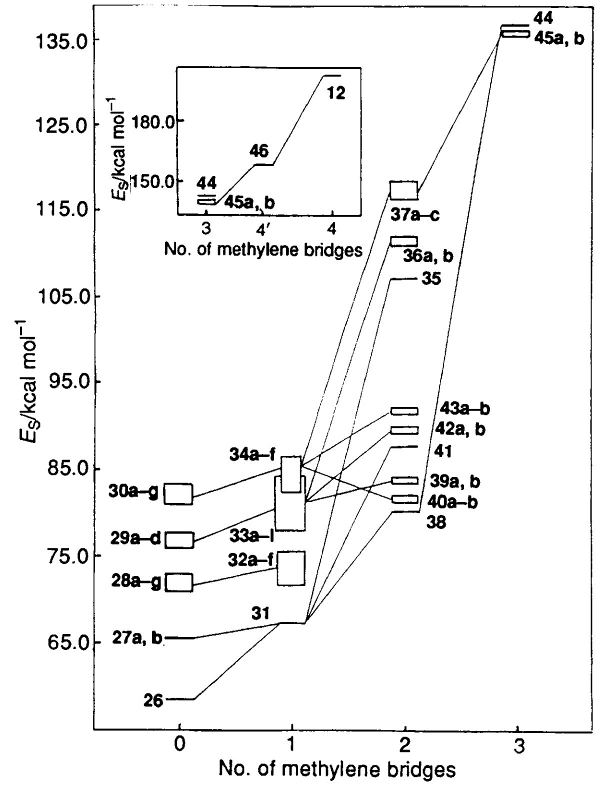

Fig. 3 Strain energy build-up on placement of methylene bridges. All the positional isomers are given as a block, the width of the block indicating the variation of strain energy depending on the position of the methyl group(s). To save space, the change in the strain energy between **44** and **12** is given in inset. 4′ denotes three methylene and one ethano bridge.

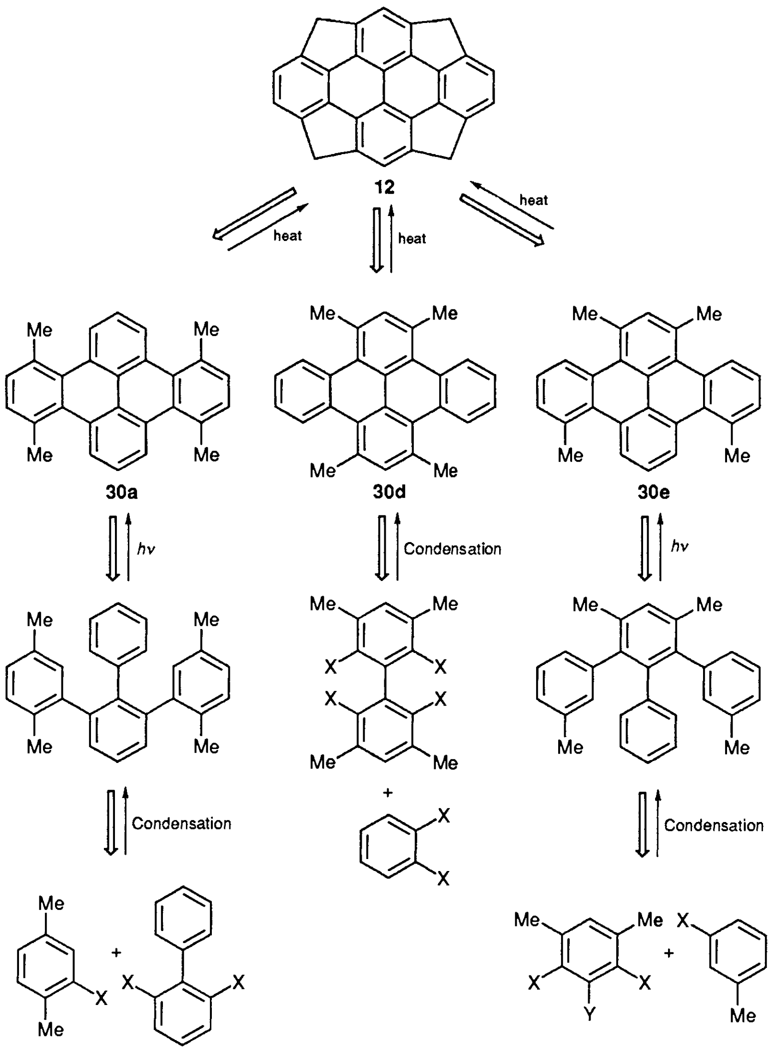

Scheme 2

bowl-shaped (**12**) geometries. **12a** has two negative frequencies (-139, -69 cm^{-1}) and the direction of the higher imaginary frequency is towards **12**, which is a minimum.* **12a** is calculated to be 48.6 kcal mol^{-1} higher in energy. Pinakene **12**, is thus a very rigid bowl compared to corannulene, **7**, and sumanene, $C_{21}H_{12}$.[4]

In **26**, the central C–C bond, *a*, is the longest (1.465 Å). **12a** is obtained by bridging with four methylene groups. The bond lengths of **12a** are stretched on the periphery (*i.e.*, *f*, *h*, *i*) and compressed on the inside (*i.e.*, *a–e*, *g*) compared with **26**. The newly formed C–CH_2 bonds (*j*, *k*) are extremely long. But in going from **12a** to **12**, the stretching of the peripheral bonds is reduced and these come closer to regular C–C bond lengths (Table 2). The constraints on the internal C–C bonds (*a–e*, *g*) are released in going from planar to bowl shape (Table 2). Stretching the peripheral bonds and compressing the inside bonds to abnormal limits is a consequence of mixing five- and six-membered rings in the planar geometry. Therefore the molecule adopts a bowl shape which releases strain.

Strain Energy Build-up in Sequential Placement of Methylene Bridges in the construction of $C_{28}H_{14}$.—Our synthetic strategy towards **12** envisaged the sequential formation of methylene bridges on methyl substituted dibenzo[*fg*,*op*]naphthacene, $C_{24}H_{14-n}Me_n$ [$n = 0$–4]. The build-up of strain energy involved in increasing the number of methylene bridges starting from unsubstituted **26** is also estimated. For each bridged or unbridged structure, several isomers are possible depending on the number of methyl groups and their position. Table 3 gives the strain energies of all isomers of methyl derivatives and mono-, di- and tri-methylene bridged dibenzo[*fg*,*op*]naphthacene molecules with varying numbers of methyl groups. In a sequential strategy, it is better to incorporate more strain in the initial stages. We are mainly interested in identifying the pathway which distributes strain evenly in all the steps. We have used a localized structure for all conjugated six-membered rings in the molecular mechanics calculations so that these may be easily compared to previous studies on C_{60} fragments.[4]

The numbering used in Table 3 is described below. The basic skeleton with hydrogens at all positions is dibenzo[*fg*,*op*]naphthacene, **26**. **27**, **28**, **29** and **30** are mono-, di-, tri- and tetramethyl derivatives of dibenzo[*fg*,*op*]naphthacene, respectively. **31** is monomethylene-bridged dibenzo[*fg*,*op*]naphthacene and the corresponding mono-, di- and tri-methyl monobridged derivatives are **32**, **33** and **34**, respectively. Three types of dibridging are possible here: **35**, **38** and **41**. The corresponding monomethyl derivatives are **36**, **39** and **42**, and dimethyl derivatives are **37**, **40** and **43**, respectively. Only one tribridged complex, **44**, is possible, and its monomethyl derivative is **45**. Various positional isomers of methyl groups are possible and the letters **a**, **b**, **c**, *etc.*, are used to distinguish them.

---

* Attempts to get a transition state (only one negative frequency) have so far led to either **12** or **12a**.

The strain energy difference between **26** and **12** is about 148 kcal mol^{-1}. Fig. 3 gives the increase in strain energy by the addition of methyl groups and methylene bridges systematically until the formation of the third bridge. Formation of the fourth bridge involves prohibitively large strain and an alternative pathway is given in the inset of Fig. 3. The differences in energy among the various isomers are very small and hence are represented as a block. Addition of each methyl group to the unbridged structure contributes up to 5–7 kcal mol^{-1}, depending on the position of the methyl groups. Therefore the strain energy difference between the tetramethyldibenzo[*fg,op*]naphthacene, **30**, and $C_{28}H_{14}$, **12**, is only 124 kcal mol^{-1}. The increase in the strain energy due to the addition of methyl groups gradually decreases as the number of bridges increases. Ultimately, in the tribridged compound, the addition of methyl groups does not add on any strain (**44** going to **45**); in fact it decreases slightly. The strain energy difference between the tetramethyl, unbridged structure **30** and the tribridged complex **45** is about 54 kcal mol^{-1}.

The formation of the first methylene bridge does not add any significant strain. The difference in the strain energy among various isomers arising from the methyl positions is less than 2 kcal mol^{-1}. All the sites are equivalent for the formation of the first bridge. There are three different sites (11–10, 8–7 and 4–3) for the formation of second methylene bridge after the first bridge (14–1) is formed. If the two methylene bridges are diagonal, there is virtually no strain energy increase. In fact, there is a decrease when starting from a trimethyl derivative of mono-bridged structure, **34a–f** (Table 3). This is due to the reduction in the non-bonded repulsion between methyl groups and hydrogens. The formation of the second bridge at site 4–3 increases the strain energy by about 8–10 kcal mol^{-1} (Table 3). The highest increase in the strain energy results in the formation of a second bridge at the 11–10 position. Approach to the tribridged structure from the monobridged structure may be easier from this high energy dibridged structure.

The increase in strain in the formation of the fourth bridge is the maximum and this could be a major impediment. An alternative pathway would be to introduce an intermediate step to divide the total strain increase into two parts. One possible way to accomplish this is initially to install an ethano bridge which can be subjected to ring contraction protocols (inset of Fig. 3). This additional synthetic step going from the trimethylene bridged compound is promising in terms of strain energy build up.

Synthetic Strategies.—The foregoing discussion of strain factors during the methano bridging process, enables delineation of a synthetic plan towards pinakene, **12**, and ultimately towards C_{70} through retrosynthetic analyses. Three key precursors, **30a**, **30d** and **30e**, are readily identified which can be assembled in a few steps from simple starting materials as shown in Scheme 2. It is expected that thermolysis of **30a**, **30d** and **30e** will lead to sequential placement of methano bridges as predicted on the basis of calculations. The scheme has the advantage that it can be readily adapted towards the placement of one or two ethano groups in place of the methano group to alleviate prohibitive build-up of strain during the bridging step. Synthetic efforts are presently underway to implement the projections made in Scheme 2.

Acknowledgements

G. N. S. thanks the Council of Scientific and Industrial Research, New Delhi, for a Senior Research Fellowship.

References

1 (*a*) W. Kratschmer, L. D. Lamb, K. Fostiropoulos and D. R. Huffman, *Nature (London)*, 1990, **347**, 354; (*b*) A. Rosen and B. Wastberg, *J. Am. Chem. Soc.*, 1988, **110**, 8701; (*c*) R. E. Haufler, J. Conceicao, L. P. F. Chibante, Y. Chai, N. E. Byrne, S. Flanagan, M. M. Haley, S. C. O'Brien, C. Pan, Z. Xiao, W. E. Billups, M. A. Ciufolini, R. H. Hauge, J. L. Margrave, L. J. Wilson, R. F. Curl and R. E. Smalley, *J. Phys. Chem.*, 1990, **94**, 8634; (*d*) L. P. F. Chibante, A. Thess, J. M. Alford, M. D. Diener and R. E. Smalley, *J. Phys. Chem.*, 1993, **97**, 8696; (*e*) C. L. Fields, J. R. Pitts, M. J. Hale, C. Bingham, A. Lweandowski and D. E. King, *J. Phys. Chem.*, 1993, **97**, 8701.

2 (*a*) H. W. Kroto, A. W. Allaf and S. P. Balm, *Chem. Rev.*, 1991, **91**, 1213; (*b*) R. F. Curl and R. E. Smalley, *Sci. Am.*, 1991, **265**, 54; (*c*) Special Issue on Buckminsterfullerenes: *Acc. Chem. Res.*, 1992, **25**, issue 3.

3 (*a*) M. D. Newton and R. E. Stanton, *J. Am. Chem. Soc.*, 1986, **108**, 2469; (*b*) G. E. Scuseria, *Chem. Phys. Lett.*, 1991, **180**, 451; (*c*) J. Baker, P. W. Fowler, P. Lazzeretti, M. Malagoli and R. Zanasi, *Chem. Phys. Lett.*, 1991, **184**, 182; (*d*) K. Raghavachari and C. M. Rohlfing, *J. Phys. Chem.*, 1991, **95**, 5768.

4 (*a*) G. N. Sastry, E. D. Jemmis, G. Mehta and S. R. Shah, *J. Chem. Soc., Perkin Trans. 2*, 1993, 1867; (*b*) G. Mehta, S. R. Shah and K. Ravi Kumar, *J. Chem. Soc., Chem. Commun.*, 1993, 1006.

5 (*a*) F. Diederich and Y. Rubin, *Angew. Chem., Int. Ed. Engl.*, 1992, **31**, 1101, and references cited therein; (*b*) M. M. Waldrop, *Sci. Res. News*, 1990, 161.

6 P. Magnus, D. Witty and A. Stamford, *Tetrahedron Lett.*, 1993, **34**, 23.

7 (*a*) A. H. Abdourazak, A. Sygula and P. W. Rabideau, *J. Am. Chem. Soc.*, 1993, **115**, 3010; (*b*) L. T. Scott, M. M. Hashemi and M. S. Batcher, *J. Am. Chem. Soc.*, 1992, **114**, 1920; (*c*) A. Borchardt, A. Fuchicello, K. V. Kilway, K. K. Baldridge and J. S. Siegel, *J. Am. Chem. Soc.*, 1992, **114**, 1921.

8 C. Fabre and A. Rassat, *C. R. Acad. Sci. (Paris)*, 1989, **308**, 1223.

9 (*a*) O. De Lucchi, personal communication; (*b*) F. Sbrogio, Thesis, University of Venezia, 1993.

10 M. Shen, I. S. Ignatyev, Y. Xie and H. F. Schaefer, III, *J. Phys. Chem.*, 1993, **97**, 3212.

11 (*a*) N. L. Allinger, *J. Am. Chem. Soc.*, 1977, **99**, 8127; (*b*) N. L. Allinger and Y. H. Yuh, *QCPE*, 1988, **11**, 395.

12 J. J. Novoa, M.-H. Whangbho and J. M. Williams, *Inorg. Chim. Acta*, 1992, **198**, 133.

13 (*a*) F. H. Kohnke and J. F. Stoddart, *Pure Appl. Chem.*, 1989, **61**, 1581; (*b*) J. F. Stoddart, *Nature (London)*, 1988, **334**, 10.

14 M. J. S. Dewar and W. Theil, *J. Am. Chem. Soc.*, 1977, **99**, 4599.

Paper 3/06608H
Received 4th *November* 1993
Accepted 15th *November* 1993